



Research article

Local conformations affect the histidine tag-Ni²⁺ binding affinity of BinA and BinB proteins

Sudarat Tharad¹, Chontida Tangsongcharoen², Panadda Boonserm³, José L. Toca-Herrera¹ and Kanokporn Srisucharitpanit^{2, *}

¹ Institute for Biophysics, Department of Nanobiotechnology, University of Natural Resources and Life Sciences (BOKU), Vienna 1190, Austria

² Faculty of Allied Health Sciences, Burapha University, Chonburi, Thailand 20131

³ Institute of Molecular Biosciences, Mahidol University, Nakhon Pathom, Thailand 73170

* **Correspondence:** Email: kanokporns@go.buu.ac.th; Tel: +6638103169.

Abstract: Binary toxin (Bin) is one of the bio-larvicidal toxin produced by *Lysinibacillus sphaericus*. Two component proteins, BinA and BinB toxins are required simultaneously to exert its larvicidal activity. The binary toxin has been proposed to act initially on the susceptible cell membrane. Here, the cell membrane binding of the binary toxin was imitated via specific histidine (His)-nickel ion (Ni²⁺) chelating. The N-terminal His-conjugated binary toxins (His-Bin) were attached onto the Ni²⁺-lipid bilayer surface besides its facilitating of purification process. The N-terminal conjugation of histidine tag did not interfere with the folding structure of both toxins. Subsequently, the attachment of binary toxins on the lipid membrane was successful with Ni²⁺-phosphatidylcholine (POPC)/phosphatidylethanolamine (POPE) bilayers (a model membrane that mimics the mosquito cell membrane) but not for Ni²⁺-phosphatidylcholine bilayer. However, His-BinA formed unstable attachment with Ni²⁺-POPC/POPE bilayers since it could be removed by buffer rinsing. In contrast, His-BinB required imidazole solution to detach from Ni²⁺-POPC/POPE. Particularly, His-BinB had higher binding affinity to Ni²⁺-ion than His-BinA. The lipid membrane attachment led to the initial finding that although BinA and BinB toxins share high homology structures, their capability for Ni²⁺ chelation was different. The local N-terminal structure of binary toxin seems to interfere the His-Ni²⁺ chelating of His-BinA.

Keywords: *Lysinibacillus sphaericus*; binary toxin; histidine tagged protein; nickel ion chelating; quartz crystal microbalance with dissipation (QCM-D)

1. Introduction

Lysinibacillus sphaericus (*Ls*) produces the binary toxin (Bin). Bin toxin is one of the bio-insecticidal toxins that has been increasingly used to control the mosquito vectors. Bin toxin is composed of 41-kDa BinA and 52-kDa BinB proteins, which are acting together for the toxicity function [1,2]. The levels of mosquito susceptibility depend on its species together with the recognition of toxin receptor [3]; highest toxicity to *Culex* spp. (vectors of West Nile virus and encephalitis), moderately active against *Anopheles* spp. (vectors of malaria), and no toxic to *Aedes* spp. (vectors of Dengue virus) [4]. However, an increase in the use of the toxins, and therefore, their long-term application have mainly led to the risk of insect resistance. The mechanism of this resistance is involved in the receptor binding of Bin toxin on larval mid gut cells [5,6,7]. A GPI-anchored protein, *C. pipiens* maltase 1 (Cpm1) on an apical cell membrane was identified as the receptor of BinB toxin [8,9]. The receptor binding of BinB has supposed to be the initial step of cell internalization of BinA-BinB co-complex [10] and the mitochondria-mediated apoptosis is subsequently observed [11,12].

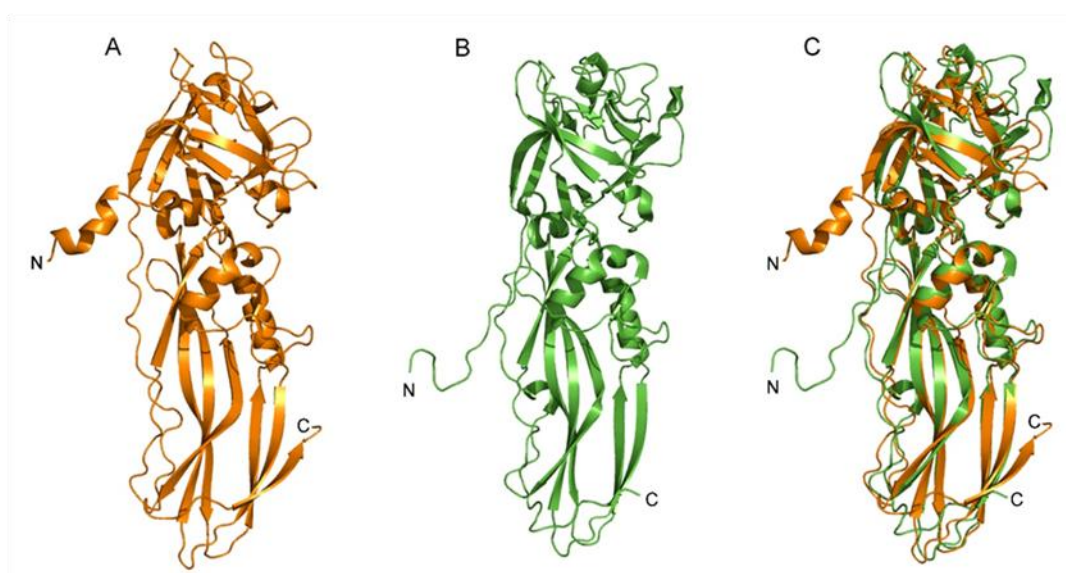


Figure 1. Three-dimensional crystal structure of binary toxins. (A) BinA structure (Protein Data Bank number, PDB: 5foy), (B) BinB structure (PDB: 3wa1) and (C) Superimposed structure of BinA and BinB.

Amino acid sequences of BinA and BinB are highly homologous with 25% identity and 40% similarity of their amino acid sequences implying a similar folding structure [13] (Supporting data 1). Recently, X-ray crystal structures of BinA and BinB proteins were resolved and confirmed their high homologous structure (Figure 1). The N-terminal domain (trefoil domain) is highly conserved to some sugar binding proteins whereas the C-terminal domain (β -sheet domain) is similar to aerolysin toxins, a β -pore forming toxin [14,15]. Up to date, the function of each domain of the binary toxin has not been identified. The toxic mechanism of binary toxin has been proposed to (i) receptor binding of BinB, (ii) BinA-BinB co-complexation for cell internalization and (iii) pore formation to release toxic unit into cytoplasm. However, the studies about the function of binary toxins have been

limited because of the receptor requirement to initiate the lipid membrane binding. The lipid bilayer may provide a suitable condition for further steps of the toxic mechanism of the binary toxin, such as BinA-BinB interaction and lipid membrane insertion. In this work, the cell membrane binding of binary toxin was mimicked via histidine (His)-nickel ion (Ni^{2+}) chelating. The His-tag was conjugated at N-terminus of both binary toxin, His-BinA and His-BinB. On the other hand, the Ni^{2+} was introduced on the lipid membrane surface with a specific lipid of DGS-NTA(Ni^{2+}). Besides the proposed lipid-membrane binding, these results firstly reveal that although Bin toxins share their protein folding structure, their binding ability of His-NTA(Ni^{2+}) on the lipid bilayers were different. Particularly, His-BinB interacts with Ni^{2+} -ion stronger than His-BinA. The local N-terminal structure of BinA has been supposed to interfere the His- Ni^{2+} chelating process.

2. Materials and Methods

2.1 Recombinant BinA and BinB proteins expression

The binary toxin from *L. sphaericus* strain 2297 was expressed as a recombinant protein. Histidine tag (6xHis) was conjugated at the N-terminus of BinA (His-BinA) and BinB (His-BinB). Both recombinant proteins were expressed by *E. coli* BL21(DE3) pLysS cells as described in previous report [16]. Briefly, the cultured cells were induced with 0.2 mM isopropyl β -D thiogalactopyranoside (IPTG) at OD₆₀₀ of 0.7 and further grown at 18 °C for 5 hours. The cultured cells were harvested by centrifugation at 7,000 g for 10 minutes. The cell pellets were suspended in the Tris-buffered saline (TBS) pH 8.0 (50 mM Tris-HCl and 200 mM NaCl), and subsequently subjected to ultra-sonication to break the cells. The soluble His-BinA and His-BinB were separated by centrifugation at 12,000 g for 1 hour and kept for further purification.

2.2 Histidine-tagged binary toxin purification

Prior metal affinity chromatographic purification, the crude protein solutions were filtrated through 0.45 μm membrane. Then, the supernatants were loaded into a precharged Ni^{2+} column (HiTrap Chelating HP 5-ml column, GE Healthcare Life Sciences) that was pre-equilibrated with Tris-buffered saline (TBS) pH 8.0. The excess of binding and non-specific bound proteins were subsequently removed with 25 mM and 50 mM imidazole-TBS. His-Bin proteins were eluted from Ni^{2+} column with imidazole gradient solution in a concentration range from 50 mM to 250 mM at a flow rate of 1 ml/min (ÄKTA, GE Healthcare Life Sciences). The eluted proteins were collected as separated fractions. Finally, the column was washed with 500 mM imidazole-TBS. Each fraction was further analyzed by 12% sodium dodecyl sulfate- polyacrylamide gel electrophoresis (SDS-PAGE).

For quartz crystal microbalance with dissipation (QCM-D) experiments, the protein fractions were collected and concentrated by ultrafiltration at 4 °C using a 30-kDa cutoff Centriprep column (Amicon). The residual imidazole in protein solution was removed by gel filtration. The concentrated proteins were applied into TBS-equilibrated desalting column (5-ml-HiTrap Sephadex G-25 column, GE Healthcare Life Sciences). Then, the proteins were eluted from the column by TBS injection.

To produce active protein, the purified His-BinA and His-BinB toxins were activated by trypsin (L-1-tosylamide-2-phenylethyl chloromethyl ketone-treated) (Sigma) at a trypsin:protein ratio of 1: 20 (w/w). The proteins were incubated at 37 °C for 2 hours. The proteolytic reaction was

stopped by adding 10 mM Phenylmethylsulfonyl fluoride (Sigma).

2.3 Intrinsic fluorescence measurement

The fluorescence spectra of the purified protein solution were recorded using a Jasco FP6300 spectrofluorophotometer. The protein solutions at a concentration of 20 $\mu\text{g/ml}$ were excited at 280 nm, and the emission spectra were collected from 300 nm to 500 nm at a scanning speed of 100 nm/min and emission slit of 1 nm. The presence spectrums of binary toxin were a subtracted value from a baseline value of buffer solution. The unfolded protein was used as a reference to compare changes of protein folding structure. The unfolded binary protein was prepared in 6 M Guanidine hydrochloride (Sigma).

2.4 Lipid vesicle preparation and characterization

1-palmitoyl-2-oleoyl-sn-glycero-3-phosphocholine (POPC) and 1-palmitoyl-2-oleoyl-sn-glycero-3-phosphoethanolamine (POPE) were purchased from Sigma-Aldrich. 1,2-dioleoyl-sn-glycero-3-[(N-(5-amino-1-carboxypentyl)iminodiacetic acid)succinyl] (DGS-NTA(Ni^{2+})) was purchased from Avanti. All lipids were aliquot and stored at $-20\text{ }^{\circ}\text{C}$.

The desired molar ratio of lipid mixtures was mixed in chloroform. Lipid films were formed by evaporating the organic solvent under a gentle nitrogen stream for at least 1 hour. The lipid films were hydrated above the melting transition temperature (T_m) for 2 hours with TBS. The hydrated film was intermittently vortexed during incubation until complete suspension. The vesicles were homogenized by using tip sonication with 50% duty cycle of 10 minutes (Branson sonifier). Then, the residual material was removed by centrifugation at 10,000g for 10 minutes. For pure POPC, the vesicles were repeatedly pressed through a polycarbonate membrane with a pore diameter of 50 nm by using a mini-extruder (Avanti). Before use, the vesicles size was determined by Zetasizer Nano ZS (Malvern Instrument). The vesicle solutions were stored at a temperature higher than T_m and were used within a week.

2.5 Quartz Crystal Microbalance with Dissipation (QCM-D) measurement

QCM-D experiments were carried out with Q-Sense E4 (Biolin Scientific). Lipid bilayer formation and further determination of Bin toxin-lipid interaction were performed on top of SiO_2 -coated sensor (QSX 303, Biolin Scientific). The sensors were sequentially cleaned with following steps of sonication in 2% (w/v) sodium dodecyl sulfate solution for 15 minutes and rinsing with ultrapure water (MilliQ, Merck). Then, the sensors were dried under nitrogen stream. The sensors were finally treated with UV/Ozone cleaner (Bioforce Nanosciences) for 30 minutes. The fundamental frequency (5 Hz) and the frequencies of the overtones (3, 5, 7, 9, 11, and 13) were evaluated prior running the experiment. The observed values of QCM-D results indicate the mass adsorption (ΔM) and the building of layer (a viscoelastic) on the crystal surface. The changes in frequency (ΔF) and dissipation (ΔD) values were real time recorded simultaneously upon materials introduced into the QCM-D chamber. The ΔF proportionally relate to the mass adsorption following Sauerbrey equation: $\Delta M = -C(\Delta f/n)$, where C corresponds to the mass sensitivity constant of the crystal sensor with $17.7\text{ ngcm}^{-2}\text{Hz}^{-1}$ and n is the overtone number. The presented ΔF data is expressed as a normalized frequency ($\Delta f/n$). The ΔD value specifies the viscoelasticity of adsorbed

layers on the surface sensor following an energy dissipation equation: $D = E_d / (2\pi E_s)$. Low ΔD values characterize the formation of a rigid layer whereas the high values relate to softer layers. The presence values correspond to the 5th overtone unless otherwise stated.

To form lipid bilayers, the QCM-D sensors were incubated with TBS under flow conditions, with a flow rate of 50 $\mu\text{l}/\text{min}$ until reach to a stable baseline (at least 1 hour). Then, 0.1 mg/ml lipid vesicle solutions were slowly filled into the QCM-D chamber with flow rate of 50 $\mu\text{l}/\text{min}$. The lipid bilayer formation was indicated by changes of ΔF and ΔD values. After that, the excess vesicle was removed by buffer rinsing until reaching a stable baseline. The binary toxins were introduced into the system at flow rate of 50 $\mu\text{l}/\text{min}$ and then the flow was paused for protein binding until the signals were stable. His-Bin toxins were eluted from Ni^{2+} -lipid bilayer by imidazole-TBS solution at the flow rate of 50 $\mu\text{l}/\text{min}$. The experiments were carried out at 25 $^\circ\text{C}$.

3. Results and Discussions

3.1 Effect of histidine-tag on the tertiary structure of binary toxins

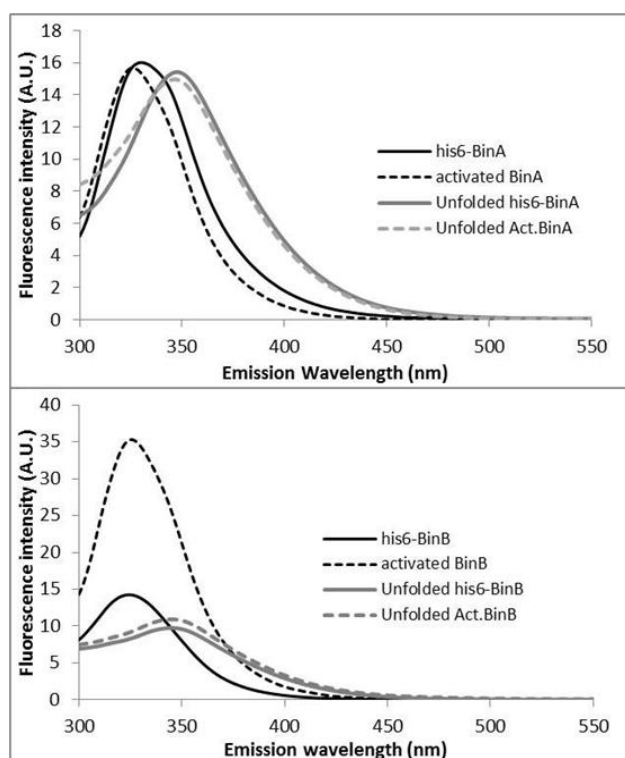


Figure 2. Intrinsic spectrum of folding structure of binary toxins. Fluorescence spectra of the binary toxin. The proteins were excited at 280 nm. The emission spectra were recorded from 300 nm to 550 nm. Upper panel and lower panel are the fluorescence spectra profiles of BinA and BinB, respectively.

The tertiary conformation (folding state) of the binary toxin was analyzed by intrinsic fluorescence spectroscopy. The purified proteins of approximately 20 $\mu\text{g}/\text{ml}$ were excited at 280 nm and fluorescence emission spectra were recorded from 300 nm to 550 nm. The interfering of the

histidine tag at N-terminus of binary toxin (His-BinA and His-BinB) could be determined from shift of emission spectrum. The activated binary toxin (native folding protein without histidine tag) showed a similar maximum spectrum at 326 nm. The presence of the histidine tag on the binary toxin structure did not significantly change the emission spectrum of the binary toxin. The emission maximum was detected at 320 nm and 324 nm for His-BinA and His-BinB, respectively. On the contrary, the unfolded BinA and BinB proteins (with and without histidine tag) showed a shift in the spectrum towards 350 nm (Figure 2). This result suggests that the overall folding structure of His-BinA and His-BinB have no deleterious effect by histidine tagged sequence. No spectrum shift was detected for His-Bin proteins when compared to the native folded protein.

3.2 Interaction of His-BinA and His-BinB with Ni²⁺-lipid bilayers

The binary toxin has been proposed to bind to a protein receptor on susceptible cell membranes as the initial step for its toxicity. In this experiment, the cell membrane binding of the binary toxin was imitated via histidine (His)-nickel ion (Ni²⁺) chelating. To approach the binary toxins onto the lipid surface, a his-tag was conjugated at N-terminus of both BinA and BinB (designed to His-BinA and His BinB) whereas DGS-NTA(Ni²⁺) lipid was included into the lipid bilayers. The phosphatidylcholine (POPC) bilayer plus 2% (mole) of DGS-NTA(Ni²⁺) lipid (Ni²⁺-POPC) was initially used as a lipid bilayer model for the binary toxin binding. The final changes of frequency value (ΔF) and dissipation value (ΔD) of Ni²⁺-POPC were about -25 Hz and 1.0×10^{-6} , respectively. These values suggest complete formation of a lipid bilayer. In addition, the lipid bilayer formation process of Ni²⁺-POPC resembled to the pure POPC case, although the maximum values of vesicle adsorption for Ni²⁺-POPC was lower than for the POPC case (supporting data 2). Protein attachment was firstly determined for His-BinB at a protein concentration of 10 $\mu\text{g/ml}$ (0.2 μM). Figure 3A shows that ΔF and ΔD values did not change implying no binding of His-BinB onto Ni²⁺-POPC bilayer. Although the protein concentration was increased to 50 $\mu\text{g/ml}$ (1.0 μM), the lipid bilayer binding was not detected. A negative control of the lipid binding was carried out with POPC bilayers which the Ni²⁺ was omitted from the lipid bilayer surface for His-protein binding. On the other hand, (negative) binding was also observed for the activated BinB (without his tag) with the Ni²⁺-POPC bilayer. The detection of the binding of BinB might be limited by either the technique sensitivity ($17.7 \text{ ngcm}^{-2}\text{Hz}^{-1}$) or an unsuitable lipid bilayer property (e.g. lipid fluidity). Taking into account the molecular weight of the binary toxin, the lipid composition probably responds to the absence of binding events. Consequently, phosphatidylethanolamine (POPE) was mixed with phosphatidylcholine (POPC) to be able to build 1:1 POPC/POPE bilayers (which mimic the mosquito cell membrane) [17]. In addition, the DGS-NTA(Ni²⁺) lipid amount was increased to 5% (mole) to overcome the limitation of surface mass detection (relate to ΔF). The 5% Ni²⁺-POPC/POPE bilayer was successfully formed as POPC and Ni²⁺-POPC bilayers (supporting data 2). Figure 3B reveals the binding of both His-BinA and His-BinB onto the Ni²⁺-POPC/POPE bilayer. On the contrary, the activated Bin toxin (without histidine sequence) was used as a negative control for histidine-Ni²⁺ chelating. As expected, the activated Bin toxin did not bind on Ni²⁺-POPC/POPE bilayer (supporting data 3). After 30 minutes of incubation, the total lipid binding of His-BinB and His-BinA were detected with $\Delta F = -30.2$ Hz and -21.9 Hz, respectively. The adsorbed mass of His-BinB and His-BinA on lipid bilayers can be calculated with the Sauerbrey relation (described in method section). The saturated binding of His-BinB and His-BinA on the Ni²⁺-POPC/POPE bilayer

resulted in an adsorbed mass of 534.5 ngcm^{-2} and 387.6 ngcm^{-2} , respectively. The detected mass of His-BinB was higher than His-BinA by approximately 27.6%. The different deposited mass between His-BinB and His-BinA might be explained by their molecular weight (MW). BinB (51 kDa) is heavier than BinA (42 kDa) [1], which corresponds to approximately 17.6%. On the other hand, similar ΔD values for His-BinA (1.9×10^{-6}) and His-BinB (1.2×10^{-6}) indicated non-significant difference in viscoelasticity between the protein-lipid hybrid layers of His-BinB and His-BinA (i.e. low ΔD values indicate a rigid layer while high values suggest a soft layer). Interestingly, His-BinA was detached from Ni^{2+} -lipid bilayer with the buffer rinsing resulting in a final $\Delta F = -6.2 \text{ Hz}$ whereas the value for His-BinB was $\Delta F = -24.6 \text{ Hz}$. After buffer rinsing, His-BinA and His-BinB were removed from the Ni^{2+} -POPC/POPE bilayers of ca. 72% and ca. 18% of total bound protein, respectively. Simultaneously, the ΔD value of His-BinA slightly decreased from 2.0×10^{-6} to 1.2×10^{-6} while the stable signal was observed for His-BinB with 1.2×10^{-6} . The ΔD value indicates a transient adsorption of His-BinA and the rigid nature of His-BinB/lipid layers. The detachment of His-BinA from Ni^{2+} -ion by buffer rinsing contradicts to a high binding affinity of (6x)histidine and Ni^{2+} ion with a dissociation constant (K_D) of $14 \times 10^{-9} \text{ M}$ [18]. On the contrary, the binding of His-BinB on Ni^{2+} -POPC/POPE bilayers followed the expectation that high affinity resists to buffer rinsing requiring imidazole for Ni^{2+} -detachment. The lower binding affinity of His-BinA also was demonstrated with the purification step. During the eluting step of protein from Ni^{2+} -column, His-BinA was eluted with 100 mM imidazole, whereas His-BinB required a higher imidazole concentration of 250 mM (Supporting data 4). These results indicate that the histidine sequence at N-terminus of BinB chelates with Ni^{2+} -ion stronger than BinA.

Although the conformational structures of BinA and BinB are highly homologous (Figure 1), a different function has been proposed for them. The X-ray crystal structure reveals the trefoil domain at N-terminus of BinA and BinB is the most different region of molecule [15]. Therefore, the N-terminal trefoil domain of BinA is supposed to interfere its Ni^{2+} -chelation efficiency. Moreover, His-BinA tends to interact with lipid membrane than BinB [19]. If the membrane interaction influences the overall structure of BinA, it is possible that the lipid bilayer may reduce the binding affinity of histidine tag together with the local structure of trefoil domain. These expectations might explain that the histidine tag at N-terminus of BinA is enough for the protein purification but not for the lipid bilayer attachment.

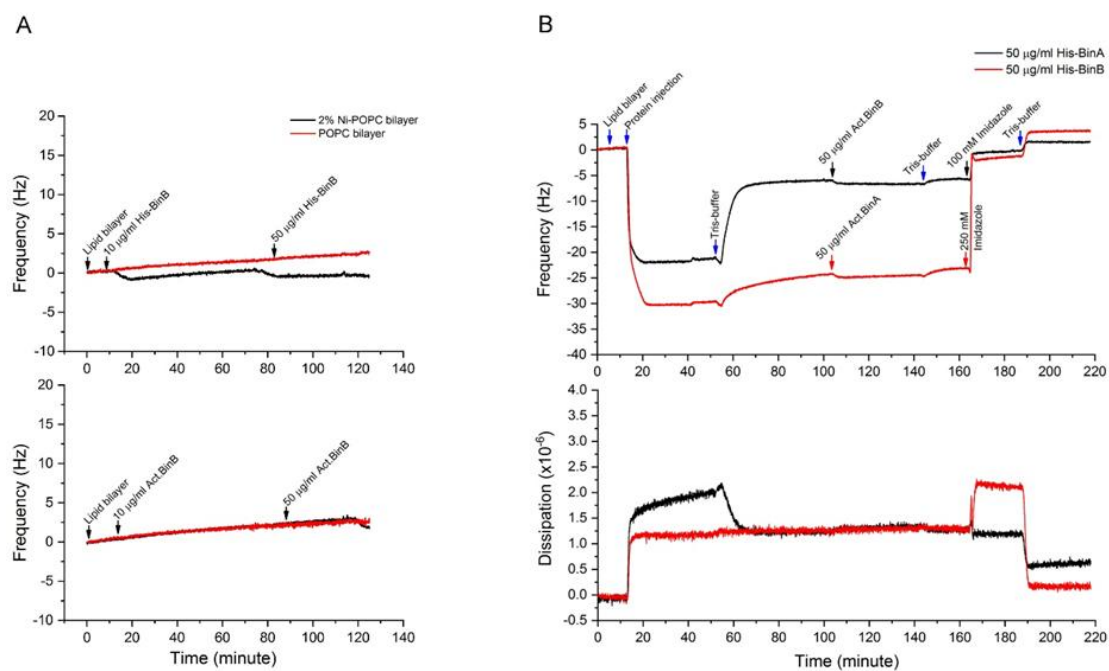


Figure 3. Interaction of binary toxins with Ni^{2+} -lipid bilayers. The lipid bilayers were formed via lipid vesicle fusion. The lipid bilayer formation is indicated as zero value at the beginning of each plot (taken as a reference for further change in frequency). The solutions were injected into the QCM-D chamber at flow rate of $50 \mu\text{l}/\text{min}$. The experiments were carried out at $25 \text{ }^\circ\text{C}$. (A) 2% (Ni^{2+})-POPC bilayers, and (B) 5% (Ni^{2+})-POPC/POPE bilayers. The blue arrow indicates to the injection of same solution whereas the black and red arrows indicate to the injection of different solutions into the system of His-BinA and His-BinB, respectively.

After protein attachment, the interaction between BinA and BinB was further investigated. The interaction was particularly demonstrated for His-BinB and activated BinA. The attachment of His-BinB on Ni^{2+} -POPC/POPE bilayer mimics the initial step of cell membrane disruption (toxicity). Later, BinA has been proposed to interact with BinB for co-internalization into the susceptible cells [10]. Figure 3B shows that activated BinA did not interact with its complementary BinB as indicated by unchanged of ΔF and ΔD signals. In addition, activated BinB showed a similar result with non-interaction with His-BinA. However, BinB could be attached on the lipid membrane via histidine- Ni^{2+} chelating (mimic the protein receptor binding on cell membranes), the interaction between BinA and BinB could not be observed. This result suggest that the BinA-BinB interaction is a complex process rather than a single protein docking mechanism on lipid surface. The change in conformational structure due to its actual protein receptor binding may trigger the BinA-BinB interaction. However, a clear evidence of BinA-BinB co-complex on lipid membranes has not been reported yet. In addition, the final rinsing step with imidazole solution resulted in decreasing of the ΔF and ΔD values closed to the zero value. This suggest the detaching of His-BinA and His-BinB from the Ni^{2+} -POPC/POPE bilayer clue in that neither BinA nor BinB insert into the lipid bilayer. The higher affinity of His-BinB, in contrast with His-BinA, was confirmed by Ni^{2+} -binding competition. The $50 \mu\text{g}/\text{ml}$ of mixed His-BinA/His-BinB solution (the final protein concentration of each is equal) was incubated with Ni^{2+} -POPC/POPE bilayer. A mixture of activated BinA and

activated BinB solution was used as a negative control (Figure 4). The final ΔF and ΔD values for His-Bin and Ni^{2+} -lipid bilayer binding were -35.1 Hz and 1.5×10^{-6} , respectively. Subsequently, Tris-buffered saline rinsing removed the non-specific bound molecules leading to a final $\Delta F = -28.2$ Hz, whereas the ΔD value remained almost constant. The protein removed from the lipid bilayer surface was about 20% of the total bound protein, which was closed to the number obtained for His-BinB (18%). In the case of His-BinA, the detached protein reached about 72%. The results suggest that His-BinB was the major protein occupying Ni^{2+} -ion on the lipid bilayer. This confirms that His-BinB has higher binding affinity against Ni^{2+} -ion than His-BinA.

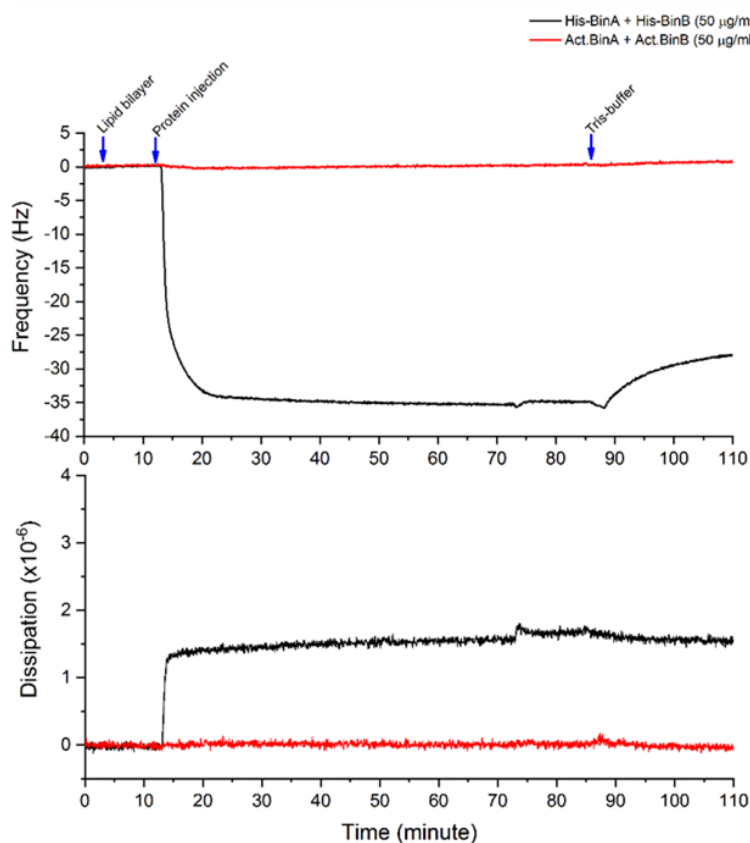


Figure 4. Binding competition of His-BinA and His-BinB onto Ni^{2+} -lipid bilayer. The protein solution containing $50 \mu\text{g/ml}$ of each His-BinA and His-BinB was incubated with 5% (Ni^{2+})-POPC/POPE bilayer for 70 minutes at 25°C . After reaching a stable baseline, the systems were rinsed with Tris-buffered saline at the flow rate of $50 \mu\text{l/min}$.

4. Conclusions

In conclusion, the histidine tag has no effect on the folding structure of binary toxin. This facilitates protein purification. Moreover, the histidine tag associates the binding of binary toxin onto the Ni^{2+} -POPC/POPE bilayer in particular for His-BinB. In contrast, His-BinA was removed from the lipid surface with buffer rinsing. Although BinA and BinB share conformational folding structure, their Ni^{2+} binding affinity were different. The trefoil domain at N-terminus of BinA has been proposed to interfere with the histidine- Ni^{2+} binding. In addition, the BinA-BinB interaction may be

triggered by its actual protein receptor rather than protein docking on lipid surface.

Acknowledgements

The authors would like to kindly thanks Monruedee Srisaisap (Mahidol University) and Jacqueline Friedmann (BOKU) for technical supporting. This work was supported by the Thailand Research Fund (TRF, MRG5980076), the Austrian Science Fund (FWF) (grant number P29562-N28), and the faculty of Allied Health Sciences, Burapha University.

Conflict of interest

The authors declare no conflicts of interest.

References

1. Baumann L, Baumann P (1989) Expression in *Bacillus subtilis* of the 51- and 42-kilodalton mosquitocidal toxin genes of *Bacillus sphaericus*. *Appl Environ Microbiol* 55: 252–253.
2. Baumann P, Clark MA, Baumann L, et al. (1991) *Bacillus sphaericus* as a mosquito pathogen: properties of the organism and its toxins. *Microbiol Mol Biol Rev* 55: 425–436.
3. Romão TP, de Melo Chalegre KD, Key S, et al. (2006) A second independent resistance mechanism to *Bacillus sphaericus* binary toxin targets its alpha-glucosidase receptor in *Culex quinquefasciatus*. *FEBS J* 273: 1556–1568.
4. Lacey LA, Undeen AH (1986) Microbial control of black flies and mosquitoes. *Annu Rev Entomol* 31: 265–296.
5. Oliveira CMF, Silva-Filha MH, Nielsen-Leroux C, et al. (2004) Inheritance and mechanism of resistance to *Bacillus sphaericus* in *Culex quinquefasciatus* (Diptera: Culicidae) from China and Brazil. *J Med Entomol* 41: 58–64.
6. Darboux I, Pauchet Y, Castella C, et al. (2002) Loss of the membrane anchor of the target receptor is a mechanism of bioinsecticide resistance. *Proc Natl Acad Sci* 99: 5830–5835.
7. Darboux I, Charles JF, Pauchet Y, et al. (2007) Transposon-mediated resistance to *Bacillus sphaericus* in a field-evolved population of *Culex pipiens* (Diptera: Culicidae). *Cell Microbiol* 9: 2022–2029.
8. Silva-Filha MH, Nielsen-LeRoux C, Charles JF (1999) Identification of the receptor for *Bacillus sphaericus* crystal toxin in the brush border membrane of the mosquito *Culex pipiens* (Diptera: Culicidae). *Insect Biochem Mol Biol* 29: 711–721.
9. Darboux I, Nielsen-LeRoux C, Charles JF, et al. (2001) The receptor of *Bacillus sphaericus* binary toxin in *Culex pipiens* (Diptera: Culicidae) midgut: molecular cloning and expression. *Insect Biochem Mol Biol* 31: 981–990.
10. Lekakarn H, Promdonkoy B, Boonserm P (2015) Interaction of *Lysinibacillus sphaericus* binary toxin with mosquito larval gut cells: Binding and internalization. *J Invertebr Pathol* 132: 125–131.
11. Tangsongcharoen C, Chomanee N, Promdonkoy B, et al. (2015) *Lysinibacillus sphaericus* binary toxin induces apoptosis in susceptible *Culex quinquefasciatus* larvae. *J Invertebr Pathol* 128: 57–63.

12. Tangsongcharoen C, Jupatanakul N, Promdonkoy B, et al. (2017) Molecular analysis of *Culex quinquefasciatus* larvae responses to *Lysinibacillus sphaericus* Bin toxin. *PLoS One* 12: e0175473.
13. Promdonkoy B, Promdonkoy P, Wongtawan B, et al. (2008) Cys31, Cys47, and Cys195 in BinA are essential for toxicity of a binary toxin from *Bacillus sphaericus*. *Curr Microbiol* 56: 334–338.
14. Srisucharitpanit K, Yao M, Promdonkoy B, et al. (2014) Crystal structure of BinB: a receptor binding component of the binary toxin from *Lysinibacillus sphaericus*. *Proteins: Structure, Function, and Bioinformatics* 82: 2703–2712.
15. Colletier JP, Sawaya MR, Gingery M, et al. (2016) De novo phasing with X-ray laser reveals mosquito larvicide BinAB structure. *Nature* 539: 43–47.
16. Srisucharitpanit K, Inchana P, Rungrod A, et al. (2012) Expression and purification of the active soluble form of *Bacillus sphaericus* binary toxin for structural analysis. *Protein Expres Purif* 82: 368–372.
17. Marheineke K, Grünewald S, Christie W, et al. (1998) Lipid composition of *Spodoptera frugiperda* (Sf9) and *Trichoplusia ni* (Tn) insect cells used for baculovirus infection. *FEBS Lett* 441: 49–52.
18. Knecht S, Ricklin D, Eberle AN, et al. (2009) Oligohis-tags: mechanisms of binding to Ni²⁺-NTA surfaces. *J Mol Recognit* 22: 270–279.
19. Chooduang S, Surya W, Torres J, et al. (2018) An aromatic cluster in *Lysinibacillus sphaericus* BinB involved in toxicity and proper in-membrane folding. *Arch Biochem Biophys* 660: 29–35.



AIMS Press

© 2020 the Author(s), licensee AIMS Press. This is an open access article distributed under the terms of the Creative Commons Attribution License (<http://creativecommons.org/licenses/by/4.0>)